Development 140, 267-279 (2013) doi:10.1242/dev.084996

FGF4 is required for lineage restriction and salt-and-pepper distribution of primitive endoderm factors but not their initial expression in the mouse

Minjung Kang[1,2], Anna Piliszek[1,*,‡], Jérôme Artus[1,*,§] and Anna-Katerina Hadjantonakis[1,¶]

SUMMARY

The emergence of pluripotent epiblast (EPI) and primitive endoderm (PrE) lineages within the inner cell mass (ICM) of the mouse blastocyst involves initial co-expression of lineage-associated markers followed by mutual exclusion and salt-and-pepper distribution of lineage-biased cells. Precisely how EPI and PrE cell fate commitment occurs is not entirely clear; however, previous studies in mice have implicated FGF/ERK signaling in this process. Here, we investigated the phenotype resulting from zygotic and maternal/zygotic inactivation of *Fgf4*. *Fgf4* heterozygous blastocysts exhibited increased numbers of NANOG-positive EPI cells and reduced numbers of GATA6-positive PrE cells, suggesting that FGF signaling is tightly regulated to ensure specification of the appropriate numbers of cells for each lineage. Although the size of the ICM was unaffected in *Fgf4* null mutant embryos, it entirely lacked a PrE layer and exclusively comprised NANOG-expressing cells at the time of implantation. An initial period of widespread EPI and PrE marker co-expression was however established even in the absence of FGF4. Thus, *Fgf4* mutant embryos initiated the PrE program but exhibited defects in its restriction phase, when lineage bias is acquired. Consistent with this, XEN cells could be derived from *Fgf4* mutant embryos in which PrE had been restored and these cells appeared indistinguishable from wild-type cells. Sustained exogenous FGF failed to rescue the mutant phenotype. Instead, depending on concentration, we noted no effect or conversion of all ICM cells to GATA6-positive PrE. We propose that heterogeneities in the availability of FGF produce the salt-and-pepper distribution of lineage-biased cells.

KEY WORDS: FGF, Blastocyst, Epiblast, Inner cell mass, Primitive endoderm, Cell lineage commitment, Live imaging

INTRODUCTION

Mammalian preimplantation development is a critical period resulting in the commitment to, and segregation of, pluripotent versus extra-embryonic lineages. The implanting mouse blastocyst comprises three spatially and molecularly distinct cell lineages. The trophectoderm (TE) forms an epithelium that encloses a fluid-filled cavity, termed the blastocoel, and an inner cell mass (ICM). The ICM is itself composed of two distinct layers: an inner population of epiblast (EPI) cells and a superficial layer of primitive endoderm (PrE) positioned adjacent to the blastocyst cavity. After implantation, the EPI will go on to form most of the embryo proper as well as extra-embryonic mesoderm (Gardner and Papaioannou, 1975; Gardner and Rossant, 1979). PrE contributes descendants to the visceral and parietal yolk sacs as well as gut endoderm (Gardner and Rossant, 1979; Gardner, 1982; Gardner, 1984; Kwon et al., 2008; Plusa et al., 2008; Viotti et al., 2011; Viotti et al., 2012). The TE produces the fetal portion of the placenta (Rossant and Tamura-Lis, 1981; Rossant and Croy, 1985).

The mechanisms by which EPI and PrE precursors arise and segregate are beginning to be elucidated, and it is now believed that allocation of cells to each of these lineages is achieved both by position within the ICM and by expression of lineage-specific transcription factors (reviewed by Artus and Hadjantonakis, 2012). Whereas all ICM cells express OCT4 (POU5F1) until the late blastocyst stage (Dietrich and Hiiragi, 2007), EPI precursors are marked by the expression of NANOG (Chazaud et al., 2006), and PrE lineage commitment and maturation are marked by the sequential activation of GATA6, SOX17, GATA4 and SOX7 (Chazaud et al., 2006; Plusa et al., 2008; Niakan et al., 2010; Artus et al., 2011).

From the morula to early blastocyst, the PrE marker GATA6 and the EPI marker NANOG are co-expressed by all cells of the embryo (Plusa et al., 2008; Guo et al., 2010). Later on, these markers progressively become mutually exclusive in their expression as lineage-biased cells emerge in a salt-and-pepper distribution within the ICM (Rossant et al., 2003; Chazaud et al., 2006; Plusa et al., 2008; Guo et al., 2010). Eventually, cells expressing markers of PrE and EPI are sorted into adjacent layers by a combination of cell movement, reinforcement of position-specific cell fate and selective apoptosis (Chazaud et al., 2006; Plusa et al., 2008; Meilhac et al., 2009; Artus et al., 2010; Morris et al., 2010; Artus et al., 2011; Frankenberg et al., 2011).

Several studies have implicated FGF/MAPK signaling in the formation of the ICM lineages in mice (reviewed by Lanner and Rossant, 2010). Embryos mutant for the downstream effector GRB2 lack PrE and exhibit pan-ICM NANOG expression at E4.5 (Cheng et al., 1998; Chazaud et al., 2006). Two recent reports demonstrated that blocking FGF signaling using specific small-molecule inhibitors also resulted in embryos that generally lack PrE cells and contain ICMs comprising exclusively NANOG-expressing cells (Nichols et al., 2009; Yamanaka et al., 2010).

[1]Developmental Biology Program, Sloan-Kettering Institute, New York, NY 10065, USA. [2]Biochemistry, Cell and Molecular Biology Program, Weill Graduate School of Medical Sciences of Cornell University, New York, NY 10065, USA.

*These authors contributed equally to this work
‡Present address: Department of Experimental Embryology, Institute of Genetics and Animal Breeding, Polish Academy of Sciences, Jastrzebiec, 05-552 Wólka Kosowska, Poland
§Present address: Institut Pasteur, CNRS URA2578, Mouse Functional Genetics Unit, 75015 Paris, France
¶Author for correspondence (hadj@mskcc.org)

Accepted 15 October 2012

Furthermore, high (and likely saturating) concentrations of exogenous FGF4 or FGF2 (bFGF) have been shown to shift the lineage balance in the opposite direction, leading to embryos with an ICM that almost exclusively comprises GATA6-expressing cells (Yamanaka et al., 2010).

Mouse embryonic stem (ES) cells, a pluripotent *in vitro* counterpart of the early EPI, are also dependent on FGF/MAPK signaling. *Fgf4* mutant ES cells can be derived and maintained in culture but fail to differentiate (Kunath et al., 2007; Stavridis et al., 2007). Blocking ERK signaling facilitates the efficient derivation of mouse ES cells and has led to the establishment of cell lines from non-permissive mouse genetic backgrounds (Hanna et al., 2009; Nichols et al., 2009) and recalcitrant species, such as the rat (Buehr et al., 2008; Li et al., 2008).

Several FGF ligands and receptors are expressed in early mouse embryos. *Fgf4* and its cognate receptor *Fgfr2* are expressed at preimplantation stages. Maternal *Fgf4* is present in the early embryo (Rappolee et al., 1994) and is zygotically produced in the EPI, but not by PrE or TE (Niswander and Martin, 1992; Rappolee et al., 1994). Conversely, *Fgfr2* is expressed by the two extra-embryonic lineages (Arman et al., 1998). Both *Fgf4* (Feldman et al., 1995; Goldin and Papaioannou, 2003) and *Fgfr2* (Arman et al., 1998) mutant embryos exhibit peri-implantation lethality that is likely to result from perturbed cell lineage allocation, and an *Fgfr2* dominant-negative mutation exhibits a failure in endoderm and ectoderm formation in embryoid bodies (Li et al., 2001). A recent study reported an inverse correlation in the expression of *Fgf4* and *Fgfr2* in ICM cells preceding the emergence of the salt-and-pepper distribution of lineage-biased ICM cells (Guo et al., 2010). Thus, reciprocal *Fgf4* and *Fgfr2* expression in prospective EPI/PrE cells presages the reciprocal expression of NANOG and GATA6 and thus could be the basis of a mechanism for lineage restriction.

Since FGF signaling has been proposed to be a crucial regulator of cell identity within the ICM, we sought to analyze the consequences of loss of *Fgf4* so as to determine the spatial and temporal requirements for this growth factor. We explored the requirement for FGF4 in both embryos with zygotic and maternal/zygotic ablation of *Fgf4* and in embryo-derived stem cells representing the lineages of the ICM. Our data revealed that FGF4 levels must be tightly regulated to generate balanced numbers of PrE and EPI progenitors within the ICM, as $Fgf4^{+/-}$ heterozygotes exhibited a reduced number of PrE cells. We noted that the onset of the PrE program, involving an initial activation of GATA6, PDGFRα and SOX17 expression, does not require FGF4. FGF4 functions in ICM lineage commitment, and a cell fate change as a response to growth factor stimulation occurs within 15 hours; however, sustained signaling activity is required to lock cells into this fate. Furthermore, application of uniform levels of FGF to *Fgf4* mutant embryos failed to restore a balanced number of EPI and PrE lineage-biased cells, suggesting that a heterogeneous supply of FGF might be required for the salt-and-pepper distribution of lineage precursors. Our data also suggest that FGF4 signaling is not necessary for later aspects of PrE maturation, at a time when a requirement within the EPI lineage promotes its transition from a naïve to a primed pluripotent state (reviewed by Nichols and Smith, 2009).

MATERIALS AND METHODS

Mouse strains

Two independently targeted *Fgf4* mutant alleles, exhibiting an identical phenotype, were used in this study and maintained on a CD1 background (Feldman et al., 1995; Sun et al., 2000). For simplicity, we have not distinguished between them in the text. Other strains used were $Fgf4^{cKO/cKO}$ and its derivative $Fgf4^{+/KO}$ (Sun et al., 2000), *Zp3:Cre* (Lewandoski et al., 1997), $Pdgfra^{+/H2B\text{-}GFP}$ (Hamilton et al., 2003) and wild-type CD1 (Charles River). Embryos with maternal and zygotic ablation of *Fgf4* were obtained by breeding $Fgf4^{KO/cKO}$; $Zp3{:}Cre^{Tg/+}$ females with $Fgf4^{KO/+}$ males. Embryos were genotyped by PCR after imaging (primers are listed in supplementary material Table S1).

Embryo collection and *in vitro* culture

Mice were maintained under a 12-hour light/dark cycle. Embryos were recovered in M2 (Millipore) and cultured in KSOM (Millipore) under mineral oil (Sigma) at 37°C and 5% CO_2 in air. For live imaging, embryos were cultured in agarose-coated glass-bottom dishes (MatTek) in an environmental chamber (Solent Scientific) as described previously (Piliszek et al., 2011). For FGF incubation experiments, FGF2 (R&D Systems) at 250-1000 ng/ml, supplemented with 1 μg/ml heparin (Sigma), was added to media. Embryos with or without a zona pellucida were cultured in micro-drops (10 embryos/15 μl drop) under mineral oil.

Embryo-derived stem cell derivation and culture

ES, TS and XEN cell lines were derived from embryos collected from $Fgf4^{+/-}$ intercrosses according to standard procedures (Tanaka et al., 1998; Kunath et al., 2005; Artus et al., 2011). Embryonic day (E) 2.5 embryos were cultured for 48 hours in KSOM supplemented with FGF2. E2.5 + 48 hours and E3.5 embryos were cultured on mitotically inactivated murine embryonic fibroblast (MEF) feeder cells for 5 days in ES cell media or for 4 days in TS cell media. ES cell medium was high glucose Dulbecco's modified Eagle's medium (D-MEM, Gibco) supplemented with 15% fetal bovine serum (FBS), 0.1 mM 2-mercaptoethanol, 1 mM non-essential amino acids, 1 mM sodium pyruvate, 2 mM glutamine, 100 units/ml penicillin and 100 μg/ml streptomycin and recombinant leukemia inhibitory factor (LIF) (Mereau et al., 1993). TS cell medium was RPMI-1640 (Invitrogen) supplemented with 20% FBS, 0.1 mM 2-mercaptoethanol, 1 mM non-essential amino acids, 1 mM sodium pyruvate, 2 mM glutamine, 100 units/ml penicillin and 100 μg/ml streptomycin, 1 μg/ml heparin and 25 ng/ml FGF2. Although we used FGF2 for all experiments presented, we noted that FGF4 treatments elicited a comparable effect (data not shown).

Outgrowths were disaggregated and passaged into 24-well dishes. Medium was replaced every 2 days. Emerging TS, XEN or ES cell colonies were passaged into new 24-well plates until confluence. Cells were then cultured in the absence of MEFs and genotyped. All cells were grown at 37°C in 5% CO_2. XEN or ES cells were routinely cultured in ES cell media without or with LIF, respectively, and replated every 2 days at a 1/5 dilution.

ES cell differentiation

Prior to differentiation, ES cells were passaged on gelatin-coated dishes to remove MEF feeders. ES cells were plated at 2×10^5 cells per 35-mm dish containing gelatin-coated glass coverslips. The next day, ES cell medium was replaced with LIF-free medium containing 10% FBS or with N2B27 medium (Ying and Smith, 2003) containing 1 μM trans-retinoic acid (Sigma). Media were changed daily. Misexpression of GATA factors was performed by transfection of pCMV-Tag2-Gata4 or pCMV-Tag2-Gata6 plasmid as described previously (Artus et al., 2010). In embryoid body (EB) experiments, 10^6 ES cells were cultured in non-adherent conditions in 10-cm Petri dishes (VWR). EBs were cultured in LIF-free medium containing 10% FBS. Medium was replaced every 2 days for 5 days. EBs were processed for cryosectioning as described previously (Artus et al., 2010).

Immunostaining

The zona pellucida was removed using acid Tyrode's solution (Sigma). Embryos were fixed in 4% paraformaldehyde in PBS for 10 minutes at room temperature or overnight at 4°C, permeabilised in 0.5% Triton X-100 in PBS for 20 minutes and then blocked in 2% horse serum in PBS for 1 hour at 4°C. Immunostaining was performed as described previously (Plusa et al., 2008; Artus et al., 2010). Primary antibodies used were: anti-DAB2 at 1/200 (BD Transduction Laboratories); undiluted anti-CDX2 (BioGenex); anti-GATA4 (Santa Cruz), anti-GATA6 (R&D Systems), anti-SOX7 (R&D Systems) all at 1/100; anti-NANOG at 1/500 (CosmoBio);

anti-FOXA2 (Abcam) and anti-SOX17 (R&D Systems) at 1/400. Secondary Alexa Fluor (Invitrogen) conjugated antibodies were used at 1/500. DNA was visualized using Hoechst 33342 (5 µg/ml; Invitrogen).

Image data acquisition and processing

Laser-scanning confocal images were acquired on a Zeiss LSM 510 META. Fluorescence was excited with a 405-nm laser diode (Hoechst), a 488-nm argon laser (GFP), a 543-nm HeNe laser (Alexa Fluor 543/555) and a 633-nm HeNe laser (Alexa Fluor 633/647). Images were acquired using a Plan Apochromat 20×/NA 0.75 objective, with optical sections of 1-2 µm. Raw data were processed using Zeiss AIM/ZEN software (Carl Zeiss Microsystems) or Imaris 7.2.2 software (Bitplane). Scale bars are provided for single optical sections (2D images).

Spinning disc confocal images were acquired using Volocity 5.4 acquisition software (Perkin-Elmer) and a Perkin-Elmer RS3 Nipkow-type scan head mounted on a Zeiss Axiovert 200M with Hamamatsu C4742-80-12AG camera. GFP was excited using a 488-nm argon laser. Images were acquired using a Zeiss Plan-Neofluar 25×/0.8 DIC Korr objective; 10-20 *xy* sections were acquired, separated by 3-4 µm. Time intervals between *z*-stacks were 15 minutes, for 10-20 hours total.

Movies of time-lapse sequences were compiled and annotated using QuickTime Pro (Apple). Fluorescence quantification measurements on fixed embryo images were performed using Imaris 7.2.2 software. Nuclei were identified using the Spot option with an estimated diameter of 5-6 µm in the Hoechst channel. Identification of nuclei by the software was confirmed manually. Protein levels were analyzed as mean fluorescence intensities inside Spot regions of interest (ROIs), and were normalized by dividing by the mean fluorescence intensity in the Hoechst channel. For fluorescence quantification measurements of time-lapse movies, images were analyzed using Volocity 5.4 acquisition software. Pdgfra$^{H2B\text{-}GFP}$-positive nuclei were identified manually using the Circle tool and defined as ROIs. Protein levels were analyzed as mean fluorescence intensities inside ROIs and were normalized by subtracting the mean background point fluorescence intensity in the GFP channel. Fluorescence quantification measurements on ES cells were analyzed using Volocity software. Mitotic figures were excluded from the analysis.

RESULTS

Initial co-expression of EPI and PrE lineage-specific transcription factors occurs in the absence of *Fgf4*

We determined the localization of lineage-specific transcription factors in *Fgf4*$^{-/-}$ embryos and compared them with stage-matched *Fgf4*$^{+/-}$ heterozygotes and wild-type embryos. From the morula (~8- to 16-cell, *n*=4) to early blastocyst stages (~32-cell stage, *n*=3), both GATA6 and NANOG were present within nuclei of the majority of ICM cells of *Fgf4*$^{-/-}$ embryos (Fig. 1A-D; supplementary material Movie 1). This distribution was indistinguishable between embryos irrespective of genotype, such that GATA6 and NANOG colocalized and were broadly expressed throughout embryos up until the 32-cell stage. As far as we could determine, the levels of GATA6 and NANOG proteins appeared comparable between stage-matched embryos irrespective of genotype (data not shown; image processing details are provided in Materials and methods). Thus, until the early blastocyst stage, embryos lacking *Fgf4* did not exhibit detectable defects in either gross morphology or the localization

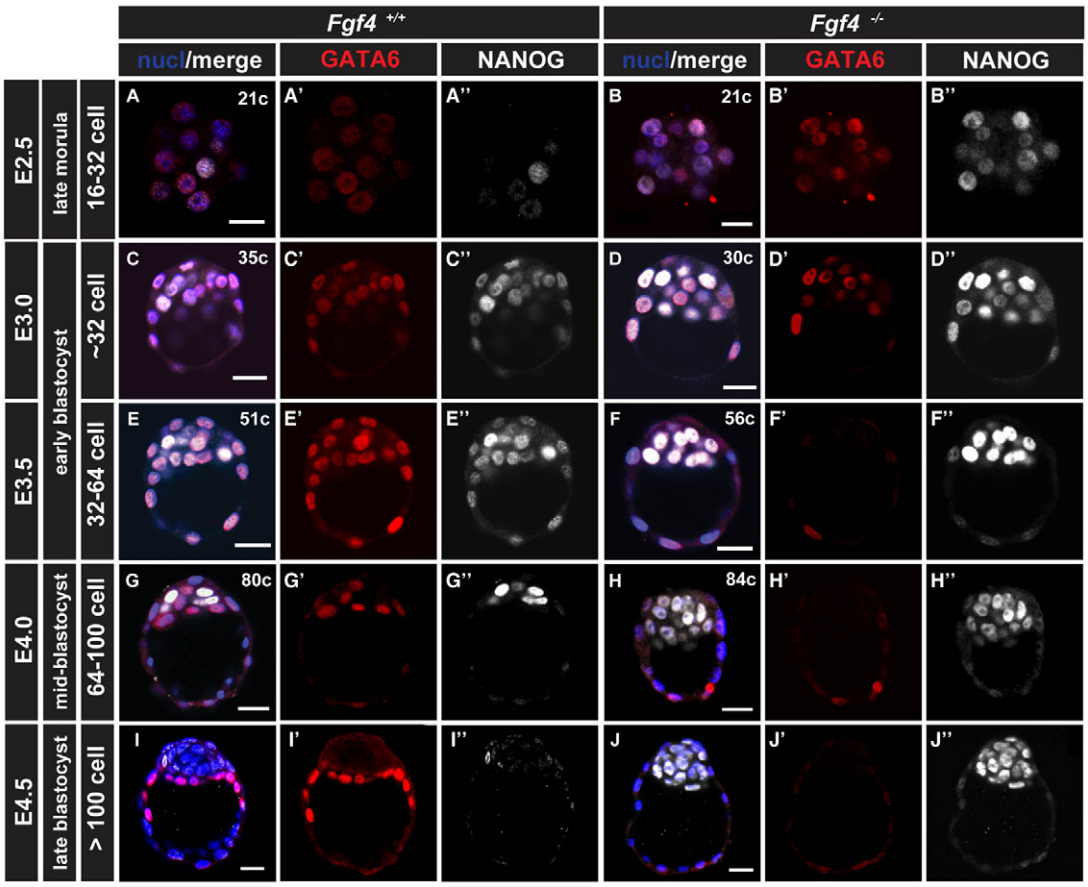

Fig. 1. *Fgf4* is not required for initial expression of GATA6 but is crucial for its PrE lineage restriction. (**A-J″**) Localization and distribution of GATA6 (red) and NANOG (white) in wild-type (*Fgf4*$^{+/+}$) and *Fgf4* mutant mouse embryos from the late morula to late/implanting blastocyst stage. Blue in merge, Hoechst. Cell numbers (c) for individual embryos are provided at the top right. Scale bars: 20 µm.

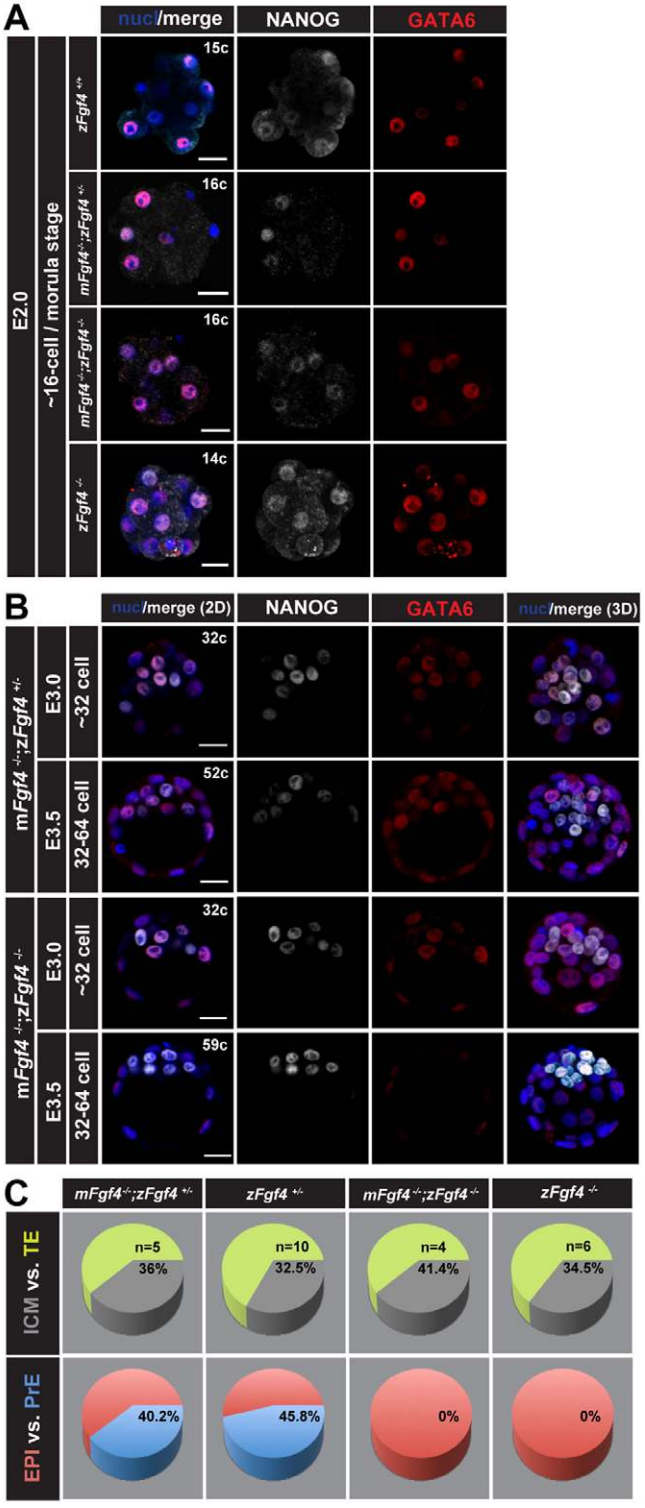

Fig. 2. Co-expression of GATA6 and NANOG in embryos lacking zygotic and maternal/zygotic *Fgf4*. (**A**) Localization of GATA6 and NANOG in wild-type, maternal, maternal/zygotic and zygotic *Fgf4* mutant embryos at the ~16-cell stage. (**B**) Localization of GATA6 and NANOG in maternal and maternal/zygotic *Fgf4* mutant embryos at the ~32-cell stage and 32- to 64-cell stage. (**C**) Statistical analysis of the lineage composition of maternal, wild-type, maternal/zygotic and zygotic *Fgf4* embryos at >80-cell stage. Wild-type, $zFgf4^{+/+}$ or $zFgf4^{+/-}$; maternal, $mFgf4^{-/-}$; $zFgf4^{+/-}$; maternal/zygotic, $mFgf4^{-/-}$; $zFgf4^{-/-}$; zygotic, $zFgf4^{+/+}$. EPI, epiblast; ICM, inner cell mass; PrE, primitive endoderm; TE, trophectoderm. Scale bars: 20 μm.

of lineage-specific transcription factors. These data suggest that the onset of GATA6 and NANOG expression is not dependent on FGF4 signaling.

FGF4 signaling is required for PrE lineage commitment

Differences between *Fgf4* mutant, heterozygous and wild-type embryos were first observed just prior to the ~64-cell stage. In wild-type embryos, GATA6 and NANOG remained broadly expressed and were overlapping in some, but not all, cells of the ICM (Fig. 1E). By contrast, in *Fgf4* mutant embryos the majority of ICM cells were NANOG positive, whereas GATA6 was weakly detected and only in a small number of cells (n=10) (Fig. 1F). $Fgf4^{-/-}$ embryos comprising more than 64 cells exhibited a blastocyst morphology, possessing an ICM and blastocoel cavity surrounded by a layer of TE. The analysis of EPI and PrE lineage-specific markers revealed profound defects within the ICM at the 64-cell stage. From this stage onward, wild-type and *Fgf4* heterozygous embryos possessed an ICM comprising NANOG-positive EPI cells and GATA6-positive PrE cells (Fig. 1E,G,I). By contrast, in *Fgf4* mutant embryos the entire ICM was composed of NANOG-positive cells, with the PrE layer missing, as confirmed by an absence of GATA6-positive cells (32- to 64-cell, n=10; 64- to 100-cell, n=3; >100-cell, n=1) (Fig. 1F,H,J). $Fgf4^{-/-}$ embryos were unable to develop past E4.5 and no embryos could be recovered at early postimplantation stages (E5.0-5.5; data not shown). These data suggest that FGF4 is required for the maintenance of GATA6 within cells of the ICM.

Maternal/zygotic and zygotic *Fgf4* mutant embryos are phenotypically indistinguishable

Since *Fgf4* has been reported to be expressed in oocytes (Rappolee et al., 1994), maternal stores could activate GATA6 prior to the 32-cell stage and in doing so obscure an earlier requirement for FGF4. To test a maternal effect, which could lead to the initiation of the PrE program, we generated maternal and zygotic (mz) *Fgf4* mutant embryos. We analyzed the localization of GATA6 and NANOG in $mzFgf4^{-/-}$ embryos and compared this with stage-matched zygotic (z) $Fgf4^{-/-}$, maternal (m) $Fgf4^{-/-}$ and wild-type embryos. At the morula (~16-cell) and early blastocyst (~32-cell) stages, both GATA6 and NANOG were present within nuclei in the majority of cells in all embryos analyzed, irrespective of genotype (total n=46; Fig. 2A; Table 1; supplementary material Movie 2). However, by the 64-cell stage, the ICM of $mzFgf4^{-/-}$ embryos contained cells that were NANOG positive and GATA6 negative, demonstrating that $mzFgf4^{-/-}$ embryos (n=4) exhibited a comparable phenotype to $zFgf4^{-/-}$ embryos (Fig. 2B). In addition, we did not observe any significant differences in lineage composition between $mzFgf4^{-/-}$ or $mFgf4^{-/-}$ embryos as compared, respectively, with $zFgf4^{-/-}$ or heterozygous embryos (Fig. 2C; P>0.05, t-test). These data suggest that there is no maternal effect of *Fgf4* and that zygotic FGF4 signaling, although required for GATA6 lineage restriction, is not involved in the initiation of GATA6 expression.

Table 1. Number of $mzFgf4^{-/-}$, $mFgf4^{-/-}$, $zFgf4^{-/-}$ and wild-type embryos analyzed at ~16-cell and ~32-cell stages

	$mzFgf4^{-/-}$	$mFgf4^{-/-}$; $zFgf4^{+/-}$	$zFgf4^{-/-}$	$zFgf4^{+/+}$
E2.0 (~16 cells)	1	9	2	8
E3.0 (~32 cells)	2	15	2	7
Total	3	24	4	15

Levels of FGF4 ensure balanced numbers of PrE and EPI cells

We next sought to determine whether the level of endogenous FGF4 quantitatively affects lineage commitment in the blastocyst (supplementary material Fig. S1). We determined the percentage of cells of each lineage – EPI, PrE and TE – in wild-type, *Fgf4* heterozygous and mutant embryos. Proportionally, there was no statistically significant difference in ICM size among the three genotypes (supplementary material Fig. S1). However, we noted a statistically significant difference in the proportion of PrE cells in $Fgf4^{-/-}$ as compared with $Fgf4^{+/-}$ and wild-type embryos (64- to 80-cell, P=0.0376; >80-cell, P=0.0135; one-way ANOVA). Although the total number of ICM cells remained constant, heterozygous embryos exhibited a reduced proportion of PrE cells (9% at the ~60- to 80-cell stage, 7% at >80-cell stage). These data suggest that not only the presence but also the dosage of FGF signaling is critical for PrE fate determination. Despite the reduced number of PrE cells within their ICM, heterozygous embryos developed normally and $Fgf4^{+/-}$ adults were recovered at Mendelian frequencies (data not shown). This suggests that mouse embryos can tolerate a significant loss of cells of the PrE lineage during early developmental stages and still develop normally to adulthood.

Failure in the sequential activation of PrE transcription factors in the absence of FGF4

Formation of the PrE involves the sequential activation of four PrE-specific transcription factors: GATA6, SOX17, GATA4 and SOX7 (Chazaud, 2008; Plusa et al., 2008; Artus et al., 2011). Activation of the second PrE-specific factor, SOX17, occurs in a time window between the 32- and 64-cell stages, when embryos are transitioning from overlapping to mutually exclusive expression of GATA6 and NANOG, concomitant with the salt-and-pepper distribution of lineage-biased cells (Morris et al., 2010; Niakan et al., 2010; Artus et al., 2011). GATA4 marks the onset of GATA6 and NANOG mutual exclusion, corresponding to the time of lineage restriction, and is activated at the ~64-cell stage, while SOX7 is activated in sorted PrE cells positioned on the surface of the ICM adjacent to the blastocoel cavity. We therefore sought to determine whether post-GATA6 markers of the PrE were activated in $Fgf4^{-/-}$ embryos. SOX17 was detected in significantly fewer cells in $Fgf4^{-/-}$ than in wild-type embryos (Fig. 3A). At the 32- to 64-cell stage, when wild-type embryos activate SOX17 expression in a subpopulation of ICM cells (n=14; average number of Sox17-positive cells, 7.29±3.83; Table 2), $Fgf4^{-/-}$ embryos exhibited a reduced number of SOX17-positive cells in the ICM (n=7; average number of Sox17-positive cells, 1.14±2.04; Fig. 3A, arrowhead; Table 2). These data suggest that SOX17 expression was initiated but not fully activated in *Fgf4* mutant embryos. In contrast to GATA6 and SOX17, we failed to observe the expression of subsequent PrE factors, including GATA4 and SOX7, in mutant embryos (GATA4, n=2, Fig. 3B and Table 2; SOX7, data not shown). Collectively, these data reveal a requirement for FGF4 in the continuation of the PrE program.

Live imaging reveals activation then downregulation of a PrE reporter in *Fgf4* mutant embryos

Having determined that PrE lineage development is impaired in the absence of *Fgf4*, we sought to live image the dynamics of lineage-specific gene expression as well as PrE cellular behaviors using a PrE lineage-specific reporter. To date, platelet-derived growth factor receptor alpha (PDGFRα) is the earliest PrE-specific marker known after GATA6 and is detected from the 16-cell stage onwards. A $Pdgfra^{H2B\text{-}GFP}$ knock-in allele provides a single-cell resolution reporter that recapitulates endogenous PDGFRα expression. In addition, as H2B-GFP is associated with chromatin, cells can be tracked and cell death can be confirmed by observing nuclear fragmentation during live imaging (Hamilton et al., 2003; Plusa et al., 2008; Artus et al., 2010).

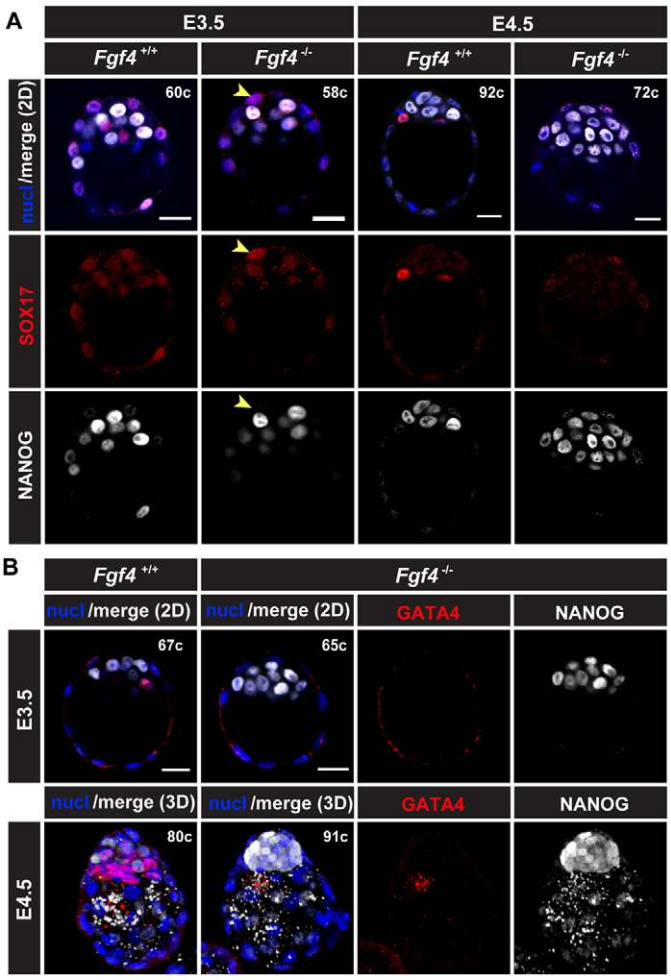

Fig. 3. Absence of FGF4 affects the expression of transcription factors activated later in the PrE program. (**A**) Localization of SOX17 and NANOG in wild-type ($Fgf4^{+/+}$) and $Fgf4^{-/-}$ embryos at E3.5 and E4.5. Arrowheads indicate SOX17-positive cells. (**B**) Localization of GATA4 and NANOG in wild-type and $Fgf4^{-/-}$ embryos at E3.5 and E4.5. Scale bars: 20 μm.

Table 2. Quantitative analysis of SOX17 and GATA4 localization in cells of wild-type and *Fgf4* mutant embryos

	Total cells in embryos	$Fgf4^{+/+}$ and $Fgf4^{+/-}$	$Fgf4^{-/-}$
SOX17			
No. of embryos	32-64	14	7
	64-100	7	2
No. of SOX17-positive cells	32-64	7.29±3.83	1.14±2.04
	64-100	8.57±2.29	0
GATA4			
No. of embryos	64-100	6	2
No. of GATA4-positive cells	64-100	9±3.74	0

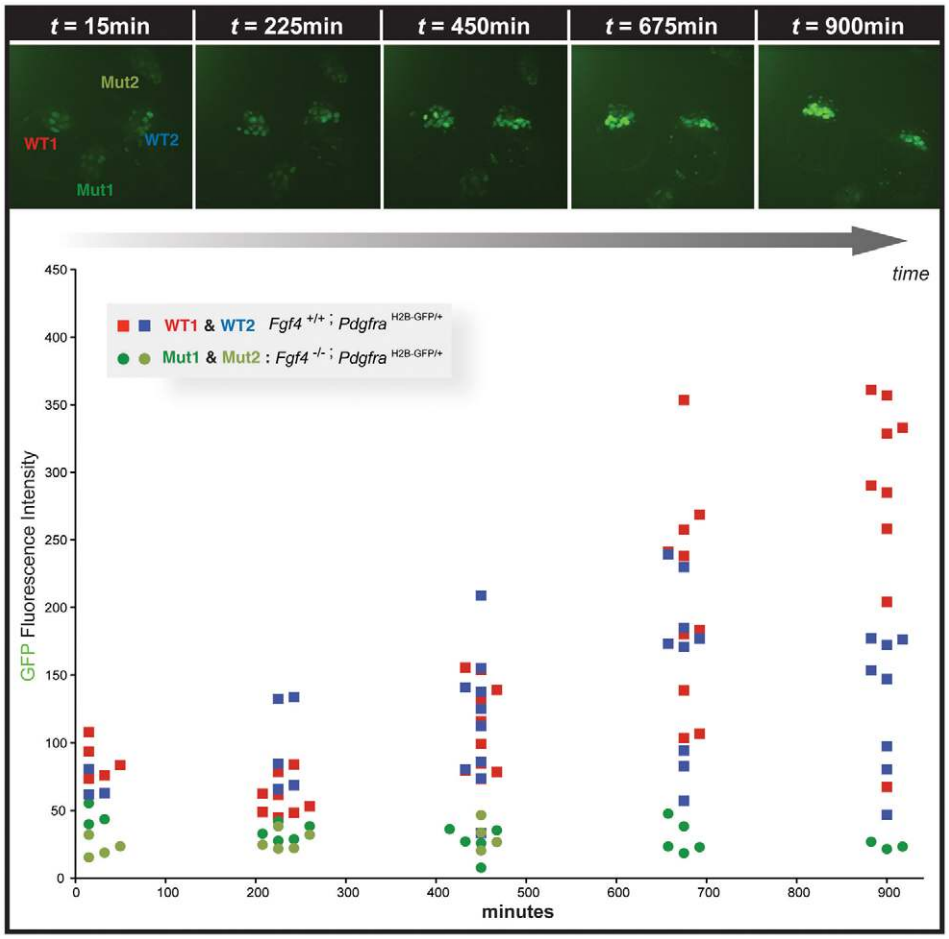

Fig. 4. Live imaging of PrE reporter dynamics in control and *Fgf4* mutant embryos. The series of panels at the top depict single time points from a 3D time-lapse movie of two wild-type (WT) and two mutant (Mut) embryos over a 900-minute period. Each point represents a maximum intensity projection of 64 μm *z*-stacks. GFP intensity was quantified in individual cells in each embryo at five time points. Beneath is shown a plot of normalized GFP fluorescence intensity over time. The four embryos are imaged in this sequence. Individual dots represent GFP-positive cells. At early time points, wild-type and mutant embryos exhibit low GFP fluorescence (*t*=15 minutes). As they develop, GFP-positive cells in wild-type embryos exhibit an increase in fluorescence intensity (*t*=225, 450 minutes). In wild-type embryos, a wide range of GFP intensity is observed (min., 46.97; max., 361.02). GFP is downregulated in mutant embryos, becoming undetectable by the end of the movie (*t*=900 minutes).

Three-dimensional time-lapse imaging of $Fgf4^{+/+}$; $Pdgfra^{+/H2B\text{-}GFP}$ embryos from early (~16- to 32-cell) to late blastocyst stages revealed an increase in the level of GFP reporter expression over time. GFP-positive cells, which were initially randomly distributed throughout the ICM, sorted into a single layer adjacent to the blastocoel (Fig. 4; supplementary material Movie 3) (Plusa et al., 2008). By contrast, live imaging of $Fgf4^{-/-}$; $Pdgfra^{H2B\text{-}GFP/+}$ embryos revealed that GFP-positive cells were initially present, but that the level of reporter expression was decreased compared with that in wild-type embryos. Then, as mutant embryos developed, fluorescent reporter expression decreased until it became undetectable (Fig. 4). Thus, the absence of PrE cells in mutant embryos is likely to occur as a result of the downregulation of PrE lineage-specific markers, such that PrE precursors fail to become committed and instead adopt an EPI fate, rather than by the elimination of these precursors and subsequent expansion of EPI-biased cells.

The kinetics of $Pdgfra^{H2B\text{-}GFP}$ reporter expression was similar to that of GATA6 in $Fgf4^{-/-}$ embryos, in which the initial expression of GATA6 was lost by the 32- to 64-cell stage (Fig. 4; supplementary material Fig. S2A). Notably, however, these observations are in contrast to previous reports in which $Pdgfra^{+/H2B\text{-}GFP}$ embryos were cultured in small-molecule inhibitors of FGF signaling. Even though the effect of such inhibitors mimics an endogenous lack of FGF signaling in $Fgf4^{+/+}$ embryos, leading to an ICM that is composed entirely of NANOG-positive cells (Nichols et al., 2009), $Pdgfra^{H2B\text{-}GFP}$ reporter expression was still observed in the 64-cell embryo and at later stages (Yamanaka et al., 2010). In our hands, $Fgf4^{+/+}$; $Pdgfra^{+/H2B\text{-}GFP}$ embryos cultured in the presence of FGF/MAPK and GSK3 (2i) inhibitors (Ying et al., 2008) produced a similar discrepancy in the dynamics of reporter expression, such that the GFP signal was detected in a number of cells throughout the ICM of embryos at the 64-cell stage and later (supplementary material Fig. S2B). As demonstrated previously (Yamanaka et al., 2010), these GFP-positive cells are GATA4 negative, suggesting that they failed to retain PrE identity, although continuing to maintain reporter expression (supplementary material Fig. S2B). In $Fgf4^{-/-}$; $Pdgfra^{+/H2B\text{-}GFP}$ embryos, the localization of GATA6 and NANOG was identical to that in inhibitor-treated wild-type embryos; however, mutant embryos did not maintain reporter expression (supplementary material Fig. S2A). This observation suggests that, although small-molecule inhibitors produce a phenotype that resembles that caused by a lack of endogenous FGF, they are not in fact identical, suggesting that small-molecule inhibitors might either elicit additional FGF4-independent effects or exert a different effect on the dynamics of lineage commitment.

Heterogeneity in $Pdgfra^{H2B\text{-}GFP}$ reporter expression suggests differential plasticity within presumptive PrE cells

Our live imaging data also revealed a wide range in fluorescence intensity among GFP-positive cells in $Fgf4^{+/+}$; $Pdgfra^{+/H2B\text{-}GFP}$ embryos, as we noted previously in static images (Plusa et al., 2008; Grabarek et al., 2012). Our time-lapse data revealed sustained differences in reporter expression as opposed to temporal fluctuations (Fig. 4). Notably, GFP-positive cells exhibited similar

behavior in embryos, increasing in fluorescence over time with the majority eventually sorting into the nascent PrE layer. We therefore propose that variations in reporter levels are likely to reflect intrinsic differences in the developmental plasticity of PrE-biased cells, as we suggested previously (Grabarek et al., 2012), although other previously described phenomena, such as reporter downregulation and apoptosis, also occur. Notably, the levels of fluorescence in *Fgf4*$^{-/-}$; *Pdgfra*$^{+/H2B\text{-}GFP}$ embryos were in the GFP-low range and then progressed to the no-GFP range, which is likely to be an indication of loss of plasticity to become PrE and restriction to the EPI lineage.

Exogenous FGF can direct all ICM cells to PrE fate in *Fgf4* mutant embryos but fails to restore balanced numbers of PrE/EPI precursors

Previous single-cell expression profiling studies revealed that the ligand *Fgf4* and the receptor *Fgfr2* are differentially expressed in early ICM cells, thereby providing a basis for generating balanced numbers of EPI and PrE progenitors (Kurimoto et al., 2006; Guo et al., 2010). Modulations of FGF signaling compromise this mutually exclusive pattern (Nichols et al., 2009; Yamanaka et al., 2010), as supported by our failure to observe a salt-and-pepper distribution of EPI/PrE lineage-biased cells in *Fgf4* mutant embryos. Considering that the programs for both ICM lineages were initiated in *Fgf4*$^{-/-}$ embryos, we hypothesized that addition of exogenous FGF to embryos cultured *ex utero* could rescue the mutant phenotype by restoring balanced numbers of EPI and PrE cells arranged in a salt-and-pepper distribution. Surprisingly, we observed that mutant embryos cultured in 250 ng/ml FGF2 from the early blastocyst (~32-cell) stage to the ~100-cell stage exhibited one of two phenotypes: the entire ICM comprised either NANOG-positive (n=4) or GATA6-positive (n=2) cells (Fig. 5Ca,b; Table 3). A comparable effect was obtained with exogenous FGF4 (data not shown).

The presence of all NANOG-positive or all GATA6-positive ICM cells in treated mutant embryos indicated that either the restoration of PrE cell fate had failed or that exogenous FGF converted all cells to a PrE identity, respectively. The failure to restore the PrE lineage in mutant embryos containing all NANOG-positive ICM cells could be due to limiting amounts of FGF2 received during culture (Fig. 5Ca). Indeed, increasing the concentration of FGF2 increased the frequency of obtaining mutant embryos with all GATA6-positive ICM cells (Fig. 5E; supplementary material Fig. S3). These data suggest that the failure of PrE lineage formation in *Fgf4*$^{-/-}$ ICM cells was not due to a defect in ICM developmental potency, but rather to the absence of an FGF signal instructing PrE commitment, which is consistent with the observation that the onset of the PrE program occurs in the mutant embryos but its restriction and maintenance are perturbed. In addition, the fact that the mutant phenotype could not be rescued by providing uniformly exogenous FGF, suggests that local heterogeneities in FGF concentration or availability link ICM lineage commitment with the emergence of a salt-and-pepper distribution of lineage-committed cells.

Time-lapse data from embryos harboring the Pdgfra$^{H2B\text{-}GFP}$ reporter exposed to exogenous FGF revealed that within 15 hours all ICM cells were GFP positive (supplementary material Movie 4). To establish if this response to FGF was transient, we cultured embryos in the presence of saturating concentrations of FGF for 24 hours, then maintained them in the absence of FGF for a further 24 hours. Mutant ICM cells did not revert to GATA6-positive cells under these conditions (Fig. 5A,D). Thus, transient exposure to the growth factor presumably elicited a transient conversion but failed to permanently restore the PrE lineage, suggesting that developmental plasticity persists and sustained signaling is required for maintenance of the PrE program (Fig. 5D). Wild-type embryos exposed to the same regimen exhibited a mutually exclusive pattern of EPI- and PrE-biased cells after culture, possibly because endogenous FGF4 was sufficient to allow the maintenance of PrE-biased cells but insufficient to convert EPI-biased cells to PrE (Fig. 5D).

Collectively, these results suggest that balanced numbers of EPI- and PrE-biased cells cannot be restored in *Fgf4*$^{-/-}$ embryos solely by the introduction of growth factor to the culture medium; rather, the non-uniform availability of FGF4, perhaps maintaining a self-reinforcing paracrine signaling loop, might be required for establishment of the salt-and-pepper distribution of lineage-biased cells.

Fgf4 is not required for the derivation or maintenance of XEN cells

Since *Fgf4* is required for PrE formation, we sought to determine whether we could derive XEN (extra-embryonic endoderm) cells from *Fgf4*$^{-/-}$ embryos. XEN cell lines have been isolated using a variety of protocols, including conditions that promote the isolation of trophoblast stem (TS) cells or ES cells (Kunath et al., 2005; Artus et al., 2010; Niakan et al., 2010). We initially attempted to isolate XEN cells from blastocyst stage embryos obtained from *Fgf4*$^{+/-}$ *inter se* crosses plated under TS derivation conditions (Fig. 6A). From 51 embryos, we successfully established 14 TS cell lines and four XEN cell lines. In our experience, the presence of exogenous FGF in TS media provides TS cells with an initial proliferative advantage over XEN cells and leads to the outcompetition of emergent XEN cells (M.K., N. Schrode and A.K.H., unpublished observations). Of the TS cell lines isolated, seven were *Fgf4*$^{-/-}$, indicating that even though TS cell maintenance requires FGF4 (Tanaka et al., 1998), TS cells can be established and maintained in the absence of endogenous FGF4

Table 3. Effects on the identity of cells within the ICM of wild-type and *Fgf4* mutant embryos after a 36-hour treatment with various concentrations of FGF

Genotype and composition of ICM following FGF treatment		Concentration of FGF (ng/ml)			
		100	250	500	1000
Fgf4$^{+/+}$ or *Fgf4*$^{+/-}$	40-60% GATA6-positive cells	2	18	1	1
	100% GATA6-positive cells	0	8	31	19
	Total	2	26	32	20
Fgf4$^{-/-}$	0% GATA6-positive cells	2	4	1	0
	40-60% GATA6-positive cells	0	0	0	0
	100% GATA6-positive cells	0	2	3	1
	Total	2	6	4	1

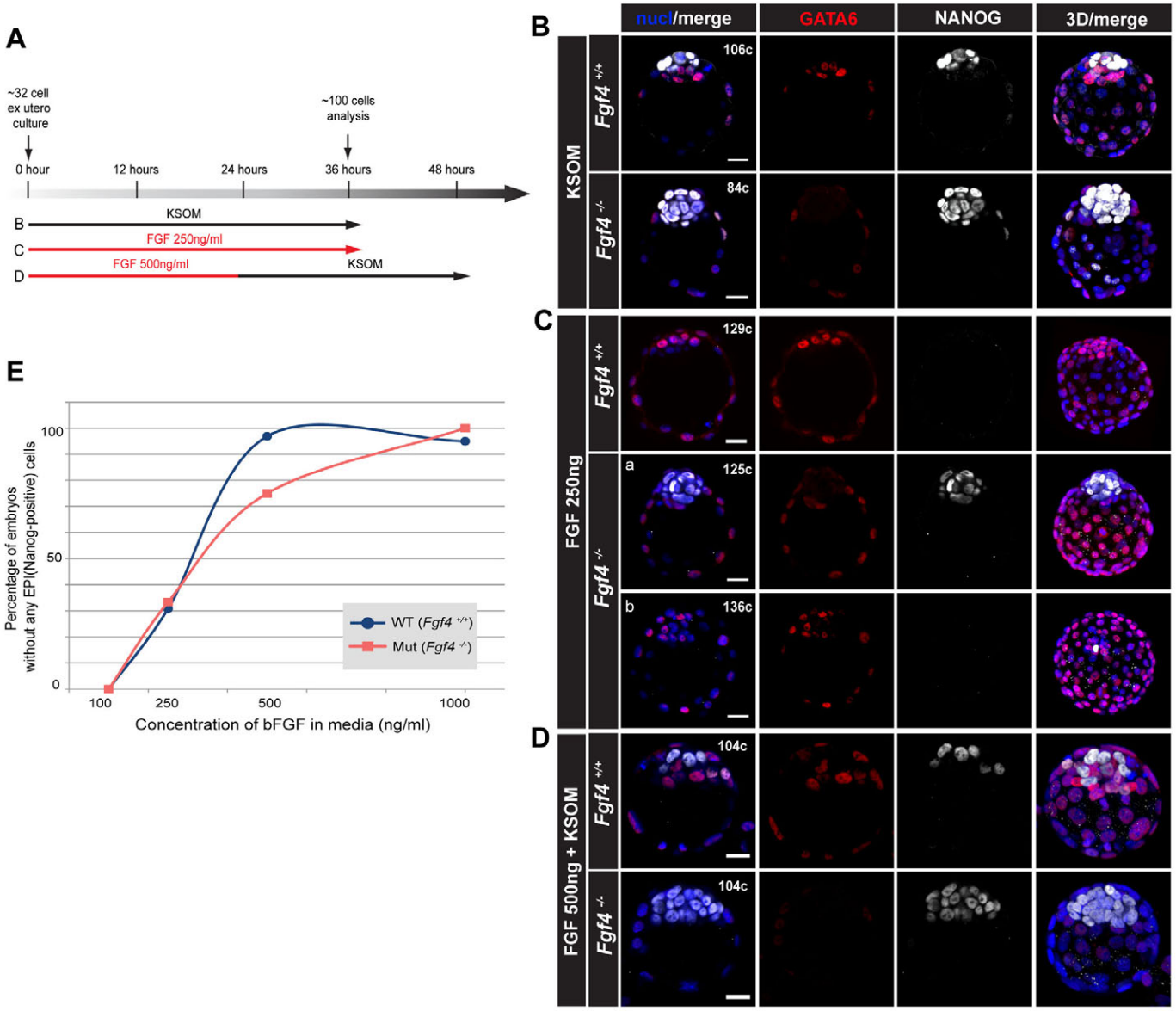

Fig. 5. Sustained exogenous FGF restores PrE cells in *Fgf4* mutant embryos but fails to rescue the mutant phenotype. (**A**) The regime for exogenous FGF treatment experiments. KSOM refers to the culture medium employed. (**B-D**) Embryos from $Fgf4^{+/-}$ intercrosses were recovered at E2.75-3.0 and cultured for 36 hours in KSOM (B), KSOM + 250 ng/ml FGF2 (C) and for 24 hours in KSOM + 500 ng/ml FGF2 followed by KSOM for 24 hours (D). (Ca) $Fgf4^{-/-}$ embryo has all NANOG-positive ICM cells; (Cb) $Fgf4^{-/-}$ embryo has all GATA6-positive ICM cells. Note that in 3D projection, GATA6 is detected in TE cells (as indicated by GATA6 staining in the outer TE cells). (**E**) Percentage of $Fgf4^{+/+}$ and $Fgf4^{-/-}$ embryos with no NANOG-positive cells after treatment with FGF2 (bFGF) over a range of concentrations. Scale bars: 20 μm.

when recombinant FGF is supplied in the culture medium. Of the four XEN cell lines that we isolated, three were $Fgf4^{+/+}$ and one was $Fgf4^{+/-}$.

We next attempted to derive XEN cell lines using an ES cell derivation protocol (Fig. 6B). From 76 blastocysts, we derived 32 ES and 11 XEN cell lines. Of the XEN cell lines that we isolated, seven were $Fgf4^{+/+}$, four were $Fgf4^{+/-}$, and none were $Fgf4^{-/-}$. Suspecting the absence of PrE cells in blastocyst embryos lacking *Fgf4* as the likely reason for our failure to isolate *Fgf4* mutant XEN cell lines, we sought to restore PrE cells in mutant embryos prior to cell line derivation by culturing $Fgf4^{-/-}$ embryos in the presence of exogenous FGF (Fig. 6C). Of 11 XEN cells derived from 80 E2.5 embryos cultured for 2 days in the presence of 250 ng/ml FGF, two were $Fgf4^{-/-}$. Mutant cells were routinely expanded and maintained in standard culture conditions and were indistinguishable from wild-type XEN cells in morphology, proliferation and marker expression (data not shown). These data suggest that, although required for PrE lineage commitment in embryos, *Fgf4* is dispensable for XEN cell propagation.

Fgf4 is not required for ES cell differentiation into PrE derivatives

Our attempts to isolate mutant XEN cell lines using an ES cell derivation protocol resulted in a relatively high number of mutant ES cell lines (Fig. 6B). This could be attributed to the presence of increased numbers of EPI cells in $Fgf4^{-/-}$ embryos. Moreover, in contrast to wild-type ICM cells in E4.5 embryos, which have downregulated NANOG, $Fgf4^{-/-}$ ICM cells

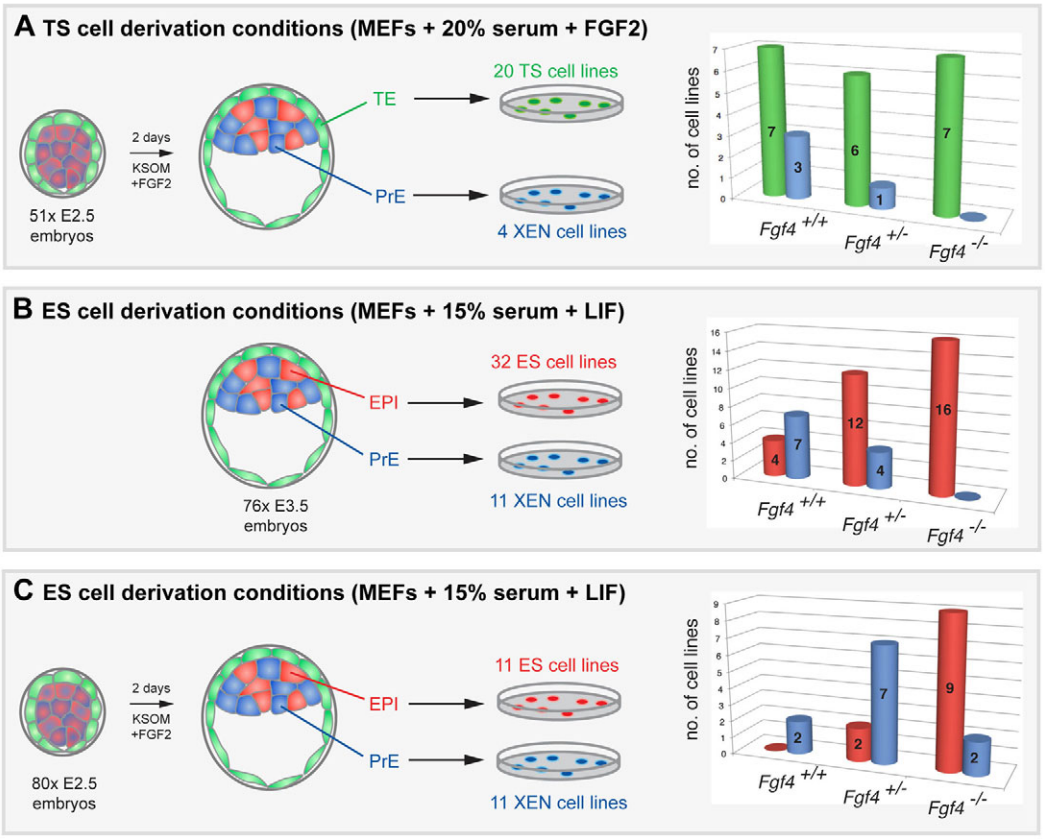

Fig. 6. XEN cells representing the PrE lineage can be isolated from *Fgf4* mutant blastocysts. Stem cell types isolated from *Fgf4*$^{+/-}$ intercross embryos using various isolation protocols. (**A**) TS and XEN cells were derived from E2.5 embryos cultured for 2 days in the presence of FGF2 using TS cell medium. (**B**,**C**) ES and XEN cells were isolated from E3.5 (B) or E2.5 (C) embryos cultured for 2 days in the presence of FGF2 using ES cell derivation conditions. The bar chart shows the representation of TS (green), XEN (blue) and ES (red) cell lines of the indicated genotypes under the different derivation conditions. MEFS, murine embryonic fibroblasts.

maintained high levels of NANOG (Fig. 1I″,J″; supplementary material Fig. S4). Elevated levels of NANOG have previously been reported in embryos cultured in the presence of FGF signaling inhibitors (Nichols et al., 2009) and in embryos mutant for the downstream effector GRB2 (Wang et al., 2011). These results suggest that EPI cells in mutant embryos might have remained in a naïve state of pluripotency that facilitates the establishment of ES cell lines, in a manner that is comparable or genetically equivalent to 2i conditions (Ying et al., 2008). Previous studies have suggested that *Fgf4*-deficient ES cells are refractory to differentiation (Kunath et al., 2007; Stavridis et al., 2007). We sought to determine whether these intrinsically naïve ES cells could differentiate into PrE derivatives and therefore whether FGF4 is required for this differentiation process.

Several protocols have been used to convert ES cells into PrE cell types. These include the misexpression of GATA4/6 (Fujikura et al., 2002; Li et al., 2004; Shimosato et al., 2007) and the generation of embryoid bodies (EBs), which differentiate an extra-embryonic endoderm (ExEn) layer on their surface (Coucouvanis and Martin, 1999). Within 48 hours of transfection with GATA4 or GATA6, we observed the upregulation of several ExEn markers including SOX17, FOXA2 and DAB2 (Fig. 7A) in wild-type, *Fgf4*$^{+/-}$ and *Fgf4*$^{-/-}$ ES cells. These data suggest that, in contrast to the early embryo, the differentiation of PrE cell types from ES cells is FGF4 independent. Alternatively, if FGF4 is epistatic to GATA factors, their misexpression would bypass its requirement, as has been shown previously for GRB2 (Wang et al., 2011).

We next sought to generate ExEn cells by differentiating EBs. After 5 days of differentiation, this cell layer was visualized by the expression of ExEn markers (Fig. 7B). This outer ExEn layer was formed normally in EBs lacking *Fgf4* and was comparable to that of *Fgf4* heterozygous and wild-type EBs. These data suggest that differentiation of ExEn cell types in EBs is independent of FGF4. Our previous data suggest that ExEn cells produced on the surface of EBs resemble the visceral endoderm of the early postimplantation embryo (Artus et al., 2010). Thus, although ES cells defective in FGF signaling are refractory in their differentiation into epiblast derivatives, our data suggest that they are still capable of forming later PrE derivatives, at least in EBs.

DISCUSSION

The emergence of EPI versus PrE precursors within the ICM of the mouse blastocyst occurs in successive phases involving initial co-expression of lineage-specific markers in all blastomeres of early embryos, subsequent mutually exclusive lineage-biased marker expression and salt-and-pepper distribution of EPI- and PrE-biased cells within the ICM (at the ~64-cell stage), followed by cell sorting to achieve lineage segregation preceding implantation (Chazaud et al., 2006; Plusa et al., 2008; Meilhac et al., 2009; Frankenberg et al., 2011).

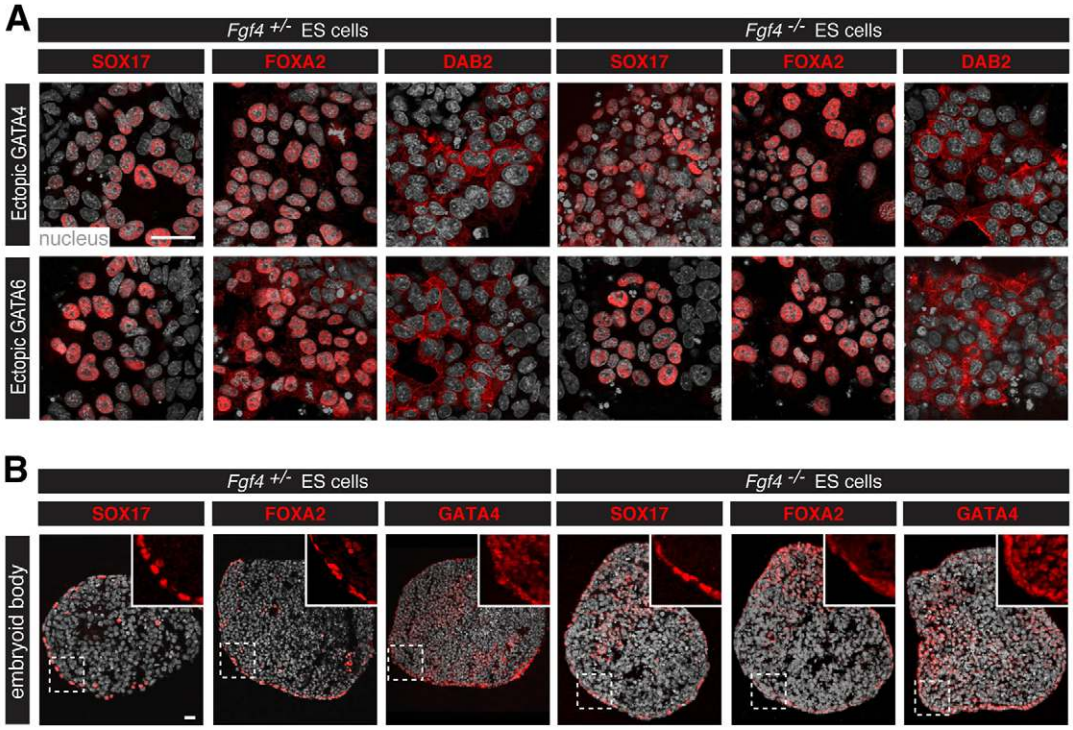

Fig. 7. Extra-embryonic endoderm differentiation of *Fgf4* mutant ES cells. (**A**) Directed differentiation of *Fgf4* heterozygous and mutant ES cells into extra-embryonic endoderm by misexpression of GATA4 and GATA6. Cells were immunostained with anti-SOX17, anti-FOXA2 and anti-DAB2 antibodies 2 days after transfection in serum-free culture conditions. Single optical sections are shown. (**B**) Cryosections of *Fgf4* heterozygous and mutant embryoid bodies at 5 days differentiation (3D reconstructions). Insets show the boxed region at higher magnification, illustrating the outer cell layer comprising extra-embryonic endoderm. Hoechst is in gray. Scale bars: 50 μm.

In this study, we investigated the requirement for FGF4 in the specification and maintenance of PrE and EPI, by analyzing the consequences of loss of FGF4 for ICM lineage specification in early mouse embryos. We observed that whereas PrE lineage restriction requires FGF4 signaling, the initiation of the PrE program does not. Indeed, both zygotic and maternal/zygotic *Fgf4* null embryos initiated co-expression of GATA6 and NANOG from the morula to 32-cell stage. Our results emphasized the absolute requirement of endogenous FGF4 signaling for the establishment of a salt-and-pepper distribution of EPI- and PrE-biased cells at the ~64-cell stage, as PrE-specific markers such as GATA6, SOX17 and PDGFRα were severely downregulated and cells instead upregulated NANOG. The PrE program cannot proceed in the absence of sustained FGF4 signaling, as illustrated by the fact that in the mutant embryos late PrE-specific markers such as GATA4 and SOX7 were not expressed (Fig. 3; data not shown) and the ICM exclusively comprised NANOG-positive cells. Interestingly, sustained FGF signaling is also required for the maturation of the EPI lineage; elevated NANOG expression was exhibited throughout the ICM in mutant embryos, suggesting that these EPI-biased cells might be kept in a naïve state and have failed to mature due to the lack of an FGF paracrine effect from PrE-biased cells.

A recent study has proposed that, during the initial stages of PrE differentiation, GATA6 is directly activated by FGF signaling from the 8-cell stage (Frankenberg et al., 2011), which is not in accordance with our observation that GATA6 expression is correctly initiated in *Fgf4*$^{-/-}$ embryos. The authors came to this conclusion based on experiments in which 8-cell to late blastocyst stage embryos were treated with FGF inhibitors. GATA6 was absent in late blastocyst stage treated embryos; however, GATA6 might still have been activated earlier on, subsequent to FGF inhibition. Accordingly, we observed that in *Fgf4* mutant embryos GATA6 cannot be maintained after the 64-cell stage (Fig. 1). In agreement with our observations, Guo and colleagues demonstrated that inhibition of FGF signaling in ~16-cell stage embryos for 24 hours did not result in a significant downregulation of *Gata6* expression, as opposed to *Pdgfra*, *Sox17* and *Gata4* (Guo et al., 2010). Therefore, we propose that, even though an inverse correlation in the expression of *Fgf4* and *Fgfr2* is established early in ICM cells, it is not involved in the colocalization of NANOG and GATA6 at the ~16- to 32-cell stage. The initial *Fgf4*-independent activation of GATA6 might result from stochastic patterning events that influence the random activation of various genes during the early stages of embryonic development (Dietrich and Hiiragi, 2007). However, our studies demonstrate that differential expression of *Fgf4* and *Fgfr2* must be sustained to produce balanced numbers of NANOG-positive and GATA6-positive cells.

Fgf4 mutant embryos can be considered FGF4 signaling nulls despite having all the machinery in place for signal transduction. Therefore, exogenous FGF can be introduced into the environment of mutant embryos to activate signaling. In this way, exogenous FGF might be expected to rescue the exclusively NANOG-positive ICM phenotype observed in mutant embryos. We favor the notion that a non-uniform concentration of FGF is required to produce ICM mosaicism; however, we cannot rule out the possibility that the absence of FGF4 results in a failure to create an early heterogeneity within the ICM, and, as a consequence, all cells exhibit a singular response to FGF. It has been proposed that NANOG expression enhances FGF4 production in a cell-autonomous manner, suggesting that the EPI-biased cells might produce localized FGF4 sources

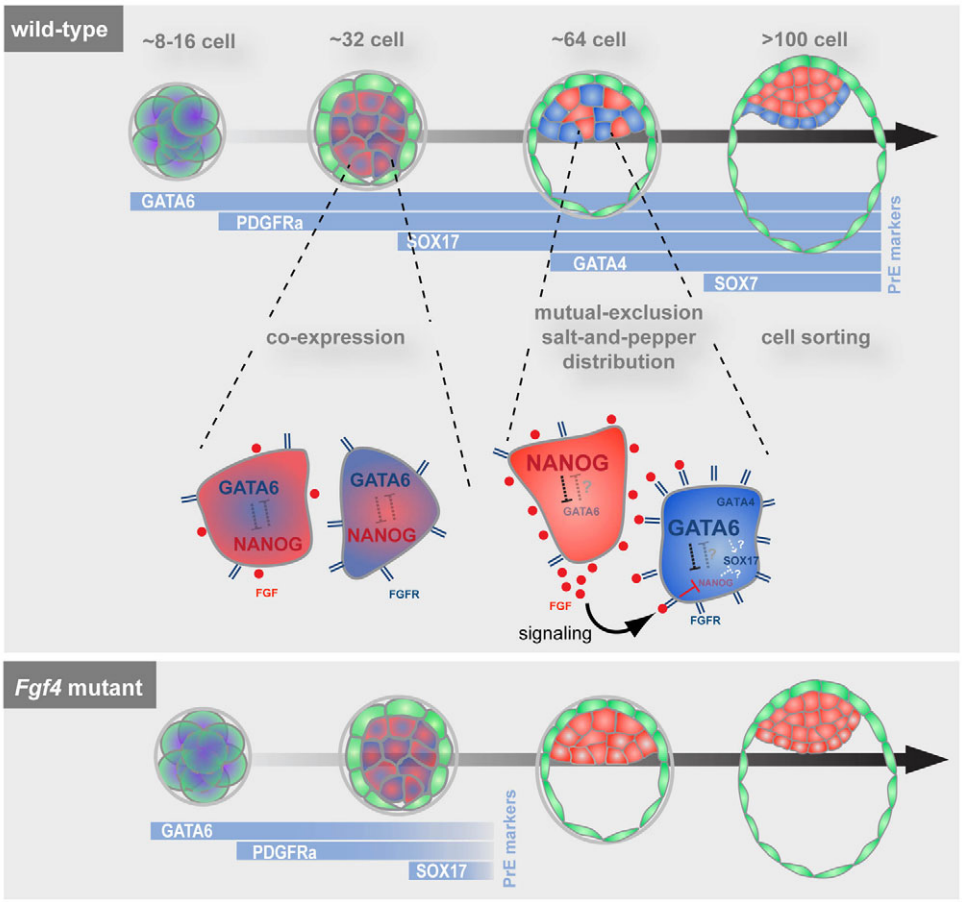

Fig. 8. Model for the role of FGF signaling in ICM lineage commitment. Differential expression levels of *Fgf4* and *Fgfr2* establish lineage biases within the ICM at the 32-cell stage. At the 64-cell stage, embryos exhibit a salt-and-pepper distribution of NANOG and GATA6 that represents the two lineages of NANOG-expressing epiblast (EPI) and GATA6-expressing primitive endoderm (PrE) lineage-biased cells. Continuous FGF4 signaling ensures lineage bias by (1) maintaining expression of the early PrE-specific factors GATA6, PDGFRα and SOX17, (2) activating the later PrE-specific factors GATA4 and SOX7, and (3) inhibiting EPI-specific factors such as NANOG. In the *Fgf4* mutant, the early PrE-specific factors GATA6, PDGFRα and SOX17 are activated but fail to be maintained, leading to a failure in PrE formation.

within the ICM (Frankenberg et al., 2011). We suggest that local heterogeneities in the availability of FGF are likely to direct neighboring ICM cells to adopt one of two alternative fates and thereafter function to stabilize them in their lineage choice.

The failure to restore balanced numbers of PrE and EPI cells in FGF-treated mutant embryos reveals a link between the reciprocal expression of FGF and FGFR at the 32-cell stage and the generation of a salt-and-pepper distribution of lineage-biased cells within the ICM at the 64-cell stage. Furthermore, although FGF signaling is not involved in the initial patterning, a cell fate change in response to FGF occurs within 15 hours, and signaling needs to be sustained for lineage choice to be locked toward a PrE fate. Interestingly, transiently incubated wild-type embryos showed a restored balance in the numbers of EPI- and PrE-biased cells after removal of exogenous FGF (Fig. 5D). These results suggest that even though all ICM cells respond to the exogenous signal and convert transiently to a PrE fate, the sustained presence of endogenous FGF signaling in wild-type embryos is sufficient to correct the imbalance after removal of the exogenous signal. The success and failure to restore balanced numbers of EPI- and PrE-biased cells in wild-type and mutant embryos, respectively, suggest that sustained and localized endogenous FGF signaling serves as a master regulator for the establishment of the mutually exclusive distribution of lineage-biased cells in the ICM.

We extended our analyses using *ex vivo* paradigms to investigate the consequences of loss of FGF signaling for embryo-derived stem cells. Using the derivation of XEN cells as a phenotypic assay, we noted that although required for ICM lineage restriction, FGF4 signaling is not necessary for later aspects of PrE biology. We successfully derived $Fgf4^{-/-}$ XEN cell lines through manipulation of the lineage bias within the ICM toward PrE cells by providing exogenous FGF. The $Fgf4^{-/-}$ XEN cells were indistinguishable from wild-type cells in their morphology, marker expression and behavior.

Our working model posits that the PrE program is activated in all blastomeres independently of FGF signaling; however, FGF signaling is then required for the restriction or maintenance of PrE cells in a subset of the ICM (Fig. 8). Heterogeneities in the availability of endogenous FGF stochastically drive lineage choice and the concomitant emergence of a salt-and-pepper distribution of lineage-biased cells within the ICM, a morphogenetic pattern that could, at least in part, be achieved through paracrine signaling. Alternatively, differential signal transduction capacity among ICM cells might be responsible for the emergence of lineage biases within the ICM (Guo et al., 2010). Further, the timing of internalization of ICM cells might lead to their differential ability to produce or transmit the FGF signal, thus promoting a signaling bias within the ICM (Morris et al., 2010).

Notably, even though FGF signaling plays a crucial role in PrE formation in the mouse, its disruption has a partial or no effect on the segregation of this lineage in early bovine or human embryos, respectively. This suggests that there are intrinsic differences in early mammalian development between species (Kuijk et al., 2012; Roode et al., 2012). Further studies will be required to elucidate the mechanism(s) driving EPI versus PrE lineage commitment in other species and to understand the evolutionary divergence from, or uniqueness of, rodents. For the time being, unanswered questions

remain in the mouse regarding the mechanisms that regulate the activation of the PrE program in early blastomeres, the inverse expression of *Fgf4* and *Fgfr2*, and the emergence of the salt-and-pepper distribution of lineage progenitors.

Acknowledgements
We thank M. Goldfarb and V. Papaioannou for *Fgf4*$^{+/-}$ ES cells; M. Lewandoski and P. Soriano for mouse strains; Y. Hayashi for GATA factor plasmids; and K. Anderson, A. Martinez-Arias, K. Niakan, B. Plusa and P. Xenopoulos for discussions and comments on the manuscript.

Funding
Work in our laboratory is supported by the Human Frontier Science Program; National Institutes of Health [RO1-HD052115 and RO1-DK084391]; and NYSTEM [C024318]. Deposited in PMC for release after 12 months.

Competing interests statement
The authors declare no competing financial interests.

Supplementary material
Supplementary material available online at
http://dev.biologists.org/lookup/suppl/doi:10.1242/dev.084996/-/DC1

References

Arman, E., Haffner-Krausz, R., Chen, Y., Heath, J. K. and Lonai, P. (1998). Targeted disruption of fibroblast growth factor (FGF) receptor 2 suggests a role for FGF signaling in pregastrulation mammalian development. *Proc. Natl. Acad. Sci. USA* **95**, 5082-5087.
Artus, J. and Hadjantonakis, A. K. (2012). Troika of the mouse blastocyst: lineage segregation and stem cells. *Curr. Stem Cell Res. Ther.* **7**, 78-91.
Artus, J., Panthier, J. J. and Hadjantonakis, A. K. (2010). A role for PDGF signaling in expansion of the extra-embryonic endoderm lineage of the mouse blastocyst. *Development* **137**, 3361-3372.
Artus, J., Piliszek, A. and Hadjantonakis, A. K. (2011). The primitive endoderm lineage of the mouse blastocyst: sequential transcription factor activation and regulation of differentiation by Sox17. *Dev. Biol.* **350**, 393-404.
Buehr, M., Meek, S., Blair, K., Yang, J., Ure, J., Silva, J., McLay, R., Hall, J., Ying, Q. L. and Smith, A. (2008). Capture of authentic embryonic stem cells from rat blastocysts. *Cell* **135**, 1287-1298.
Chazaud, C. (2008). Early embryogenesis in mammals: stem cells and first commitment steps. *Med. Sci. (Paris)* **24**, 1043-1048.
Chazaud, C., Yamanaka, Y., Pawson, T. and Rossant, J. (2006). Early lineage segregation between epiblast and primitive endoderm in mouse blastocysts through the Grb2-MAPK pathway. *Dev. Cell* **10**, 615-624.
Cheng, A. M., Saxton, T. M., Sakai, R., Kulkarni, S., Mbamalu, G., Vogel, W., Tortorice, C. G., Cardiff, R. D., Cross, J. C., Muller, W. J. et al. (1998). Mammalian Grb2 regulates multiple steps in embryonic development and malignant transformation. *Cell* **95**, 793-803.
Coucouvanis, E. and Martin, G. R. (1999). BMP signaling plays a role in visceral endoderm differentiation and cavitation in the early mouse embryo. *Development* **126**, 535-546.
Dietrich, J. E. and Hiiragi, T. (2007). Stochastic patterning in the mouse pre-implantation embryo. *Development* **134**, 4219-4231.
Feldman, B., Poueymirou, W., Papaioannou, V. E., DeChiara, T. M. and Goldfarb, M. (1995). Requirement of FGF-4 for postimplantation mouse development. *Science* **267**, 246-249.
Frankenberg, S., Gerbe, F., Bessonnard, S., Belville, C., Pouchin, P., Bardot, O. and Chazaud, C. (2011). Primitive endoderm differentiates via a three-step mechanism involving Nanog and RTK signaling. *Dev. Cell* **21**, 1005-1013.
Fujikura, J., Yamato, E., Yonemura, S., Hosoda, K., Masui, S., Nakao, K., Miyazaki Ji, J. and Niwa, H. (2002). Differentiation of embryonic stem cells is induced by GATA factors. *Genes Dev.* **16**, 784-789.
Gardner, R. L. (1982). Investigation of cell lineage and differentiation in the extraembryonic endoderm of the mouse embryo. *J. Embryol. Exp. Morphol.* **68**, 175-198.
Gardner, R. L. (1984). An *in situ* cell marker for clonal analysis of development of the extraembryonic endoderm in the mouse. *J. Embryol. Exp. Morphol.* **80**, 251-288.
Gardner, R. L. and Papaioannou, V. E. (1975). Differentiation in the trophectoderm and inner cell mass. In *The Early Development of Mammals: 2nd Symposium of the British Society for Developmental Biology* (ed. M. Balls and A. E. Wild). Cambridge, UK: Cambridge University Press.
Gardner, R. L. and Rossant, J. (1979). Investigation of the fate of 4-5 day post-coitum mouse inner cell mass cells by blastocyst injection. *J. Embryol. Exp. Morphol.* **52**, 141-152.
Goldin, S. N. and Papaioannou, V. E. (2003). Paracrine action of FGF4 during periimplantation development maintains trophectoderm and primitive endoderm. *Genesis* **36**, 40-47.
Grabarek, J. B., Zyzynska, K., Saiz, N., Piliszek, A., Frankenberg, S., Nichols, J., Hadjantonakis, A. K. and Plusa, B. (2012). Differential plasticity of epiblast and primitive endoderm precursors within the ICM of the early mouse embryo. *Development* **139**, 129-139.
Guo, G., Huss, M., Tong, G. Q., Wang, C., Li Sun, L., Clarke, N. D. and Robson, P. (2010). Resolution of cell fate decisions revealed by single-cell gene expression analysis from zygote to blastocyst. *Dev. Cell* **18**, 675-685.
Hamilton, T. G., Klinghoffer, R. A., Corrin, P. D. and Soriano, P. (2003). Evolutionary divergence of platelet-derived growth factor alpha receptor signaling mechanisms. *Mol. Cell. Biol.* **23**, 4013-4025.
Hanna, J., Markoulaki, S., Mitalipova, M., Cheng, A. W., Cassady, J. P., Staerk, J., Carey, B. W., Lengner, C. J., Foreman, R., Love, J. et al. (2009). Metastable pluripotent states in NOD-mouse-derived ESCs. *Cell Stem Cell* **4**, 513-524.
Kuijk, E. W., van Tol, L. T., Van de Velde, H., Wubbolts, R., Welling, M., Geijsen, N. and Roelen, B. A. (2012). The roles of FGF and MAP kinase signaling in the segregation of the epiblast and hypoblast cell lineages in bovine and human embryos. *Development* **139**, 871-882.
Kunath, T., Arnaud, D., Uy, G. D., Okamoto, I., Chureau, C., Yamanaka, Y., Heard, E., Gardner, R. L., Avner, P. and Rossant, J. (2005). Imprinted X-inactivation in extra-embryonic endoderm cell lines from mouse blastocysts. *Development* **132**, 1649-1661.
Kunath, T., Saba-El-Leil, M. K., Almousailleakh, M., Wray, J., Meloche, S. and Smith, A. (2007). FGF stimulation of the Erk1/2 signalling cascade triggers transition of pluripotent embryonic stem cells from self-renewal to lineage commitment. *Development* **134**, 2895-2902.
Kurimoto, K., Yabuta, Y., Ohinata, Y., Ono, Y., Uno, K. D., Yamada, R. G., Ueda, H. R. and Saitou, M. (2006). An improved single-cell cDNA amplification method for efficient high-density oligonucleotide microarray analysis. *Nucleic Acids Res.* **34**, e42.
Kwon, G. S., Viotti, M. and Hadjantonakis, A. K. (2008). The endoderm of the mouse embryo arises by dynamic widespread intercalation of embryonic and extraembryonic lineages. *Dev. Cell* **15**, 509-520.
Lanner, F. and Rossant, J. (2010). The role of FGF/Erk signaling in pluripotent cells. *Development* **137**, 3351-3360.
Lewandoski, M., Wassarman, K. M. and Martin, G. R. (1997). Zp3-cre, a transgenic mouse line for the activation or inactivation of loxP-flanked target genes specifically in the female germ line. *Curr. Biol.* **7**, 148-151.
Li, X., Chen, Y., Schéele, S., Arman, E., Haffner-Krausz, R., Ekblom, P. and Lonai, P. (2001). Fibroblast growth factor signaling and basement membrane assembly are connected during epithelial morphogenesis of the embryoid body. *J. Cell Biol.* **153**, 811-822.
Li, L., Arman, E., Ekblom, P., Edgar, D., Murray, P. and Lonai, P. (2004). Distinct GATA6-and laminin-dependent mechanisms regulate endodermal and ectodermal embryonic stem cell fates. *Development* **131**, 5277-5286.
Li, P., Tong, C., Mehrian-Shai, R., Jia, L., Wu, N., Yan, Y., Maxson, R. E., Schulze, E. N., Song, H., Hsieh, C. L. et al. (2008). Germline competent embryonic stem cells derived from rat blastocysts. *Cell* **135**, 1299-1310.
Meilhac, S. M., Adams, R. J., Morris, S. A., Danckaert, A., Le Garrec, J. F. and Zernicka-Goetz, M. (2009). Active cell movements coupled to positional induction are involved in lineage segregation in the mouse blastocyst. *Dev. Biol.* **331**, 210-221.
Mereau, A., Grey, L., Piquet-Pellorce, C. and Heath, J. K. (1993). Characterization of a binding protein for leukemia inhibitory factor localized in extracellular matrix. *J. Cell Biol.* **122**, 713-719.
Morris, S. A., Teo, R. T., Li, H., Robson, P., Glover, D. M. and Zernicka-Goetz, M. (2010). Origin and formation of the first two distinct cell types of the inner cell mass in the mouse embryo. *Proc. Natl. Acad. Sci. USA* **107**, 6364-6369.
Niakan, K. K., Ji, H., Maehr, R., Vokes, S. A., Rodolfa, K. T., Sherwood, R. I., Yamaki, M., Dimos, J. T., Chen, A. E., Melton, D. A. et al. (2010). Sox17 promotes differentiation in mouse embryonic stem cells by directly regulating extraembryonic gene expression and indirectly antagonizing self-renewal. *Genes Dev.* **24**, 312-326.
Nichols, J. and Smith, A. (2009). Naive and primed pluripotent states. *Cell Stem Cell* **4**, 487-492.
Nichols, J., Silva, J., Roode, M. and Smith, A. (2009). Suppression of Erk signalling promotes ground state pluripotency in the mouse embryo. *Development* **136**, 3215-3222.
Niswander, L. and Martin, G. R. (1992). Fgf-4 expression during gastrulation, myogenesis, limb and tooth development in the mouse. *Development* **114**, 755-768.
Piliszek, A., Kwon, G. S. and Hadjantonakis, A. K. (2011). Ex utero culture and live imaging of mouse embryos. *Methods Mol. Biol.* **770**, 243-257.
Plusa, B., Piliszek, A., Frankenberg, S., Artus, J. and Hadjantonakis, A. K. (2008). Distinct sequential cell behaviours direct primitive endoderm formation in the mouse blastocyst. *Development* **135**, 3081-3091.

Rappolee, D. A., Basilico, C., Patel, Y. and Werb, Z. (1994). Expression and function of FGF-4 in peri-implantation development in mouse embryos. *Development* **120**, 2259-2269.
Roode, M., Blair, K., Snell, P., Elder, K., Marchant, S., Smith, A. and Nichols, J. (2012). Human hypoblast formation is not dependent on FGF signalling. *Dev. Biol.* **361**, 358-363.
Rossant, J. and Croy, B. A. (1985). Genetic identification of tissue of origin of cellular populations within the mouse placenta. *J. Embryol. Exp. Morphol.* **86**, 177-189.
Rossant, J. and Tamura-Lis, W. (1981). Effect of culture conditions on diploid to giant-cell transformation in postimplantation mouse trophoblast. *J. Embryol. Exp. Morphol.* **62**, 217-227.
Rossant, J., Chazaud, C. and Yamanaka, Y. (2003). Lineage allocation and asymmetries in the early mouse embryo. *Philos. Trans. R. Soc. Lond. B Biol. Sci.* **358**, 1341-1349.
Shimosato, D., Shiki, M. and Niwa, H. (2007). Extra-embryonic endoderm cells derived from ES cells induced by GATA factors acquire the character of XEN cells. *BMC Dev. Biol.* **7**, 80.
Stavridis, M. P., Lunn, J. S., Collins, B. J. and Storey, K. G. (2007). A discrete period of FGF-induced Erk1/2 signalling is required for vertebrate neural specification. *Development* **134**, 2889-2894.
Sun, X., Lewandoski, M., Meyers, E. N., Liu, Y. H., Maxson, R. E., Jr and Martin, G. R. (2000). Conditional inactivation of Fgf4 reveals complexity of signalling during limb bud development. *Nat. Genet.* **25**, 83-86.
Tanaka, S., Kunath, T., Hadjantonakis, A. K., Nagy, A. and Rossant, J. (1998). Promotion of trophoblast stem cell proliferation by FGF4. *Science* **282**, 2072-2075.
Viotti, M., Nowotschin, S. and Hadjantonakis, A. K. (2011). Afp:mCherry, a red fluorescent transgenic reporter of the mouse visceral endoderm. *Genesis* **49**, 124-133.
Viotti, M., Niu, L., Shi, S. H. and Hadjantonakis, A. K. (2012). Role of the gut endoderm in relaying left-right patterning in mice. *PLoS Biol.* **10**, e1001276.
Wang, Y., Smedberg, J. L., Cai, K. Q., Capo-Chichi, D. C. and Xu, X. X. (2011). Ectopic expression of GATA6 bypasses requirement for Grb2 in primitive endoderm formation. *Dev. Dyn.* **240**, 566-576.
Yamanaka, Y., Lanner, F. and Rossant, J. (2010). FGF signal-dependent segregation of primitive endoderm and epiblast in the mouse blastocyst. *Development* **137**, 715-724.
Ying, Q. L. and Smith, A. G. (2003). Defined conditions for neural commitment and differentiation. *Methods Enzymol.* **365**, 327-341.
Ying, Q. L., Wray, J., Nichols, J., Batlle-Morera, L., Doble, B., Woodgett, J., Cohen, P. and Smith, A. (2008). The ground state of embryonic stem cell self-renewal. *Nature* **453**, 519-523.